Colloid and Polymer Science (2019) 297:261–269
https://doi.org/10.1007/s00396-018-04461-7

ORIGINAL CONTRIBUTION

A novel stimulus-responsive temozolomide supramolecular vesicle based on host–guest recognition

Mingfang Ma[1] · Lingdong Kong[1] · Zhongyu Du[1] · Zengyang Xie[1] · Lin Chen[1] · Ruijiao Chen[1] · Zhenquan Li[1] · Jun Liu[1] · Zhaolou Li[1] · Aiyou Hao[2]

Received: 1 August 2018 / Revised: 9 December 2018 / Accepted: 14 December 2018 / Published online: 7 January 2019

Abstract

Temozolomide is a potent chemotherapeutic agent for glioblastoma multiforme treatment. However, its low aqueous solubility and short half-life (only about 1.8 h) in plasm limit its clinical therapeutics. Herein, a supramolecular vesicle based on hydroxypropyl-β-cyclodextrin and temozolomide was firstly constructed by elaborate design and preparation, which can load temozolomide into membranous layer of vesicle effectively. The morphologies and diameters of this temozolomide-loaded vesicle were characterized through transmission electron microscope, scanning electron microscope, and dynamic light scattering. The possible vesicle formation mechanism was further studied by X-ray diffraction, Fourier transform infrared spectrum, ultraviolet-visible spectroscopy, ^{1}H nuclear magnetic resonance, and 2D nuclear magnetic resonance (ROSEY). Finally, the stimulus responsiveness of this vesicle was studied. Temozolomide can be released from the membrane of the vesicle once copper ions were dropped into the vesicle solution.

Keywords Temozolomide · Vesicle · Hydroxypropyl-β-cyclodextrin · Drug delivery

Introduction

Most of brain cancer is glioblastoma multiforme (GBM), while temozolomide (TMZ, Scheme 1) is one of the most effective drugs in GBM treatment [1]. As illustrated in Fig. 1, under physiological conditions, TMZ can hydrolyze into 5-(3-methyl-triazen-1-yl)imidazole-4-carboxamide (MTIC) [2]. Only TMZ molecules cross the blood–brain barrier, enter into GBM cells, and hydrolyze into MTIC; it can induce DNA damage of GBM cells. MTIC is inactive when it is outside of GBM cells. Unfortunately, half-life period of TMZ is very short in plasma, only about 1.8 h [3], since TMZ can degrade into MTIC in the blood. Besides, the solubility of TMZ in water is very low [4]. Those above deficiencies all limit TMZ clinical applications. Chemists have tried their best to develop drug carriers to solve those deficiencies in the past decade. Polycefin, prodrug, microemulsion, nanoparticles, liposome, and so on can all be used as drug carriers to deliver TMZ [1–8]. For example, Scherman et al. has encapsulated TMZ into the cavity of cucurbit[7]uril, prolonging the lifetime of the TMZ since encapsulation can decrease TMZ degradation under physiological conditions [9]. Moreover, encapsulation can improve TMZ activity compared to natural TMZ. Recently, Golomb et al. has successfully encapsulated TMZ into PEGylated liposome, leading longer survival of rats treated with TMZ liposomes compared to treatment with TMZ solution [10].

However, as far as we know, the supramolecular vesicle based on hydroxypropyl-β-cyclodextrin (HP-β-CD, Scheme 1) encapsulated with TMZ has not been reported yet. The vesicle containing bilayer membrane [11–14], which is similar with liposome, has been applied widely in nanoreactors,

Mingfang Ma and Aiyou Hao contributed equally to this work.

Electronic supplementary material The online version of this article (https://doi.org/10.1007/s00396-018-04461-7) contains supplementary material, which is available to authorized users.

✉ Mingfang Ma
mamingfang2012@163.com

✉ Aiyou Hao
haoay@sdu.edu.cn

[1] Laboratory of New Antitumor Drug Molecular Design & Synthesis of Jining Medical University, College of Basic Medicine, Jining Medical University, Jining 272067, People's Republic of China

[2] Key Laboratory of Colloid and Interface Chemistry of Ministry of Education & School of Chemistry and Chemical Engineering, Shandong University, Jinan 250100, People's Republic of China

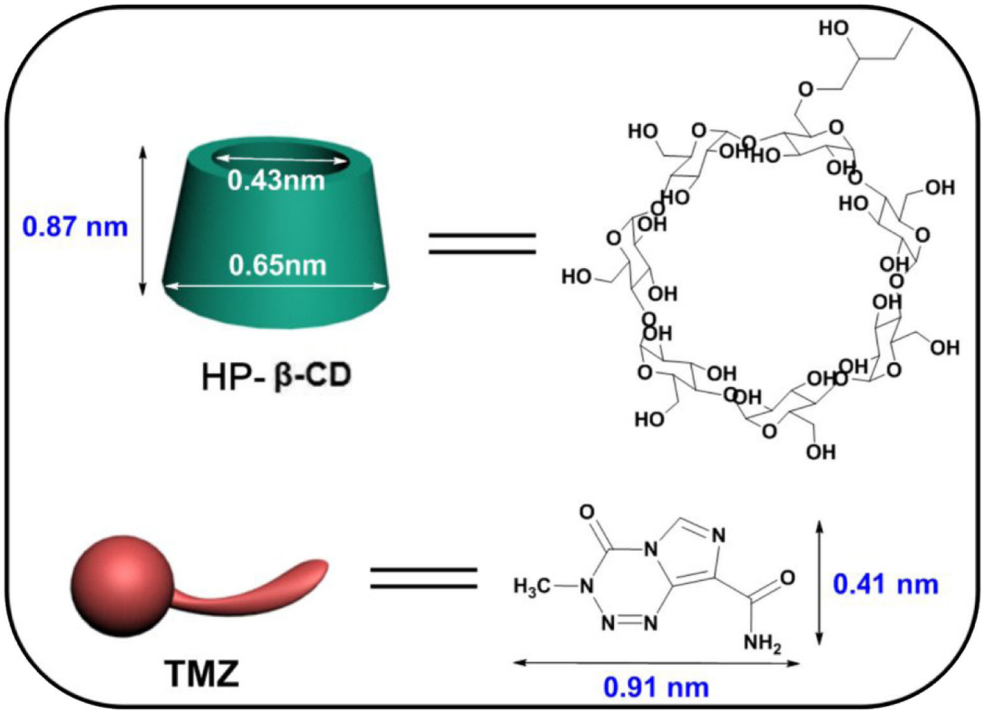

Scheme 1 Structures of hydroxypropyl-β-cyclodextrin (HP-β-CD) and temozolomide (TMZ)

template synthesis, cell membrane mimicking, and gene or drug delivery [15–19]. The supramolecular vesicle is an important branch of vesicle, which can be constructed by noncovalent interactions, consisting of π–π stacking, electrostatic forces, host–guest recognition, and charge transfer [20–24]. Supramolecular vesicle is sensitive to external stimuli, including pH, ions, electrons, enzymes, and light [25–30], endowing this colloid material with a potential application in drug delivery and release. As a drug delivery soft material, supramolecular vesicle can deliver hydrophilic drug. Liu et al. has constructed a supramolecular vesicle by host–guest recognition between p-sulfonatocalixarene and asymmetric viologen [31]. After ultracentrifugation and dialysis, doxorubicin can be successfully loaded into the interior of the vesicle. The doxorubicin-loaded vesicles show lower damage for normal cells while same antitumor activity to cancer cells in contrast with doxorubicin itself. Supramolecular vesicle can deliver hydrophobic drug as well. Our team has reported a supramolecular vesicle based on amphiphilic β-cyclodextrin [32]. Paclitaxel can be loaded into the vesicle's membrane.

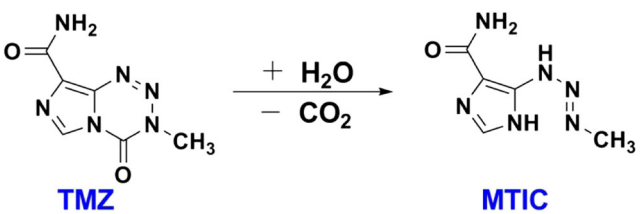

Fig. 1 Chemical structures of TMZ and MTIC

Paclitaxel-loaded vesicles exhibit remarkable anticancer activity compared to natural paclitaxel. Afterwards, we find that paclitaxel can form amphiphile with ethanediamine-arm modified β-cyclodextrin; the supramolecular amphiphile can assemble into supramolecular vesicles spontaneously [33], paving a new avenue to construct drug-loaded vesicle.

Herein, a novel stimulus-responsive TMZ supramolecular vesicle is firstly reported. β-cyclodextrin (β-CD) is a cyclic oligosaccharide, containing seven glucose units connected by α-1,4-glucosidic bond [34, 35]. β-CD has hydrophobic cavity and hydrophilic outside the surface, which can encapsulate hydrophobic molecules [36, 37]. β-CD is used widely in supramolecular chemistry because of its high water solubility, favorable biocompatibility, and easy functionalization [38, 39]. HP-β-CD is one of the most significant β-CD derivatives. The water solubility of HP-β-CD is higher than β-CD [40]. As shown in Scheme 1, the narrow diameter of HP-β-CD cavity is 0.43 nm, while the size of TMZ is 0.41 nm calculated by Materials Studio 5.5; hence, HP-β-CD can easily encapsulate TMZ. In this study, HP-β-CD can encapsulate TMZ to form supramolecular amphiphile through host–guest recognition. The obtained supramolecular amphiphile can further self-assemble into a vesicle. The diameters of HP-β-CD/TMZ vesicles mainly distribute from 200 to 240 nm in aqueous solution. Nanoparticles including vesicles can selectively accumulate in tumor by enhanced permeability and retention (EPR) effect [32]. So, our HP-β-CD/TMZ vesicles may be preferentially delivered to tumor through this passive targeting mechanism. Moreover, HP-β-CD/TMZ vesicles exhibit

sensitive stimulus responsiveness to copper ions. HP-β-CD/TMZ vesicles will change to irregular aggregates when copper ions are added into this vesicle system. Hence, our HP-β-CD/TMZ vesicle is a smart drug delivery system, which may have potential application in GBM treatment.

Experimental section

Materials

HP-β-CD was bought from Binzhou Zhiyuan Biotechnology Co. Ltd., China. TMZ and all other chemical reagents were all purchased from Sinopharm Chemical Reagent Co. Ltd., China.

Analytical instruments and methods

Transmission electron microscope (TEM) pictures were obtained through a transmission electron microscope (JEM-100CX, JEOL Ltd). Scanning electron microscope (SEM) images were carried out on a scanning electron microscope (Hitachi S-4800). Phosphotungstic acid was used to stain TEM samples for detection. TEM samples were then dried by an infrared lamp after staining. SEM samples for measurement were sprayed using gold. Ultraviolet-visible (UV-vis) spectroscopy was used to obtain UV-vis curves by a TU-1800pc UV-vis spectrophotometer (Purkinje General Co. Ltd. Beijing, China). Dynamic light scattering (DLS, Wyatt QELS Technology DAWN HELEOS instrument) was used to measure hydration radius of vesicles. Water was filtered by a 0.45-μm filter before preparation of DLS sample. A German Bruker D8ADVANCE diffractometer was used to get X-ray diffraction (XRD) spectrum. An Avatar 370 FT-IR Spectrometer was used to obtain Fourier transform infrared (FT-IR) spectrum by KBr pellet method. ^{1}H nuclear magnetic resonance (^{1}H NMR) measurement was on API Bruker Avance 300 M NMR. 2D NMR ROESY experiments were recorded by an API Bruker Avance 400M NMR. Materials Studio 5.5 by Accelrys was used to calculate the sizes of HP-β-CD and TMZ molecules.

Preparation of HP-β-CD/TMZ solid complex and their physical mixture

Through freeze-drying HP-β-CD/TMZ complex aqueous solutions, HP-β-CD/TMZ solid complex was prepared. By mixing HP-β-CD and TMZ powders directly, HP-β-CD/TMZ physical mixture was prepared. For HP-β-CD/TMZ physical mixture sample preparation of FT-IR detection, 1:1 ratio of HP-β-CD and TMZ is ground with KBr firstly, then HP-β-CD/KBr and TMZ/KBr are ground immediately.

Detection of the stoichiometries of HP-β-CD/TMZ

HP-β-CD (10^{-3} mol/L) and TMZ (10^{-3} mol/L) aqueous solutions were prepared firstly. Then different HP-β-CD/TMZ solutions with different molar ratios of 10:0, 9:1, 8:2, 7:3, 6:4, 5:5, 4:6, 3:7, 2:8, 1:9, and 0:10 were prepared. UV-vis spectrums of above solutions were detected; the max absorption peaks were picked. Finally, Job's plot was obtained.

Preparation of the vesicles

HP-β-CD (2×10^{-4} mol/L) and TMZ (2×10^{-4} mol/L) solutions were prepared firstly. Then HP-β-CD/TMZ (1×10^{-4} mol/L) solution was prepared by mixing HP-β-CD and TMZ solution in a centrifuge tube. Finally, the vesicle samples were prepared by sonicating HP-β-CD/TMZ solution for 30 min and placing for about one day. HP-β-CD/TMZ vesicles can be obtained by dialyzing HP-β-CD/TMZ solution through dialysis membrane.

Stimulus responsiveness of vesicle system

TMZ contains an amido group, so it may coordinate with copper ions. Hence, the effect of copper ions on HP-β-CD/TMZ vesicles was studied. $CuCl_2$ aqueous solution (1×10^{-4} mol/L) was prepared firstly. Then $CuCl_2$ aqueous solution was dropped into HP-β-CD/TMZ vesicles' solution. Finally, the mixed solution was sat a day at ambient temperature.

Results and discussions

Morphologies and sizes

The UV-vis absorbance of different concentrations of HP-β-CD/TMZ sample solutions was obtained by UV-vis detection as shown in Fig. S1. UV-vis absorption intensity increased along with HP-β-CD/TMZ sample's increasing concentration. The maximum absorption intensity was picked. Interestingly, the slope changed obviously when HP-β-CD/TMZ sample's concentration was above 1×10^{-4} mol/L, illustrating critical aggregate concentration of HP-β-CD/TMZ sample should be about 1×10^{-4} mol/L. So the morphology of HP-β-CD/TMZ sample at critical aggregate concentration was observed by electron microscopy. From Fig. 2a and b, we can see the obtained HP-β-CD/TMZ vesicles clearly under TEM [41]. The diameters of spherical vesicles are about 170 to 200 nm. SEM detection was further used to confirm the vesicle's existence since it can provide surface topography of aggregates. For organic material such as vesicle, it is better to be coated with gold to improve the electroconductivity for clear observation. As shown in Fig. 2c and d, aggregates with a spherical shape can be seen under SEM, which can further confirm HP-β-CD/

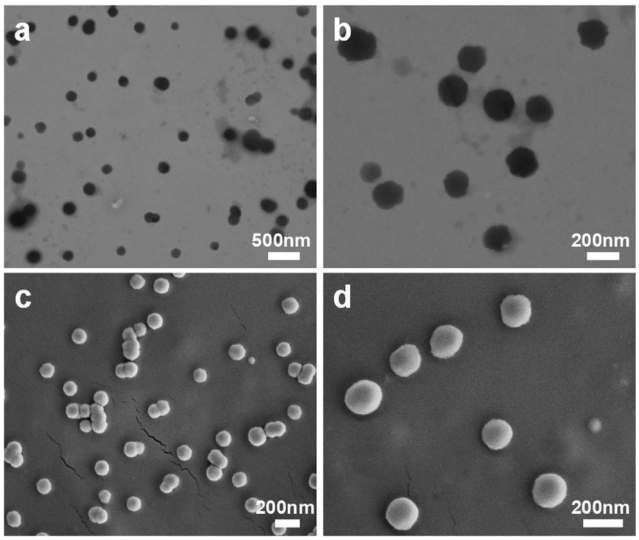

Fig. 2 HP-β-CD/TMZ vesicles' TEM and SEM images (1×10^{-4} mol/L) at room temperature, **a** TEM, scale bar = 500 nm; **b** TEM, scale bar = 200 nm; **c** SEM, scale bar = 200 nm; **d** SEM, scale bar = 200 nm

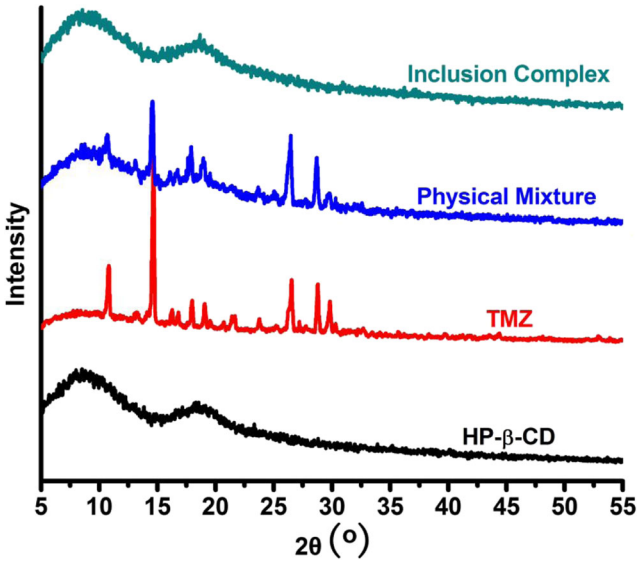

Fig. 4 XRD patterns of HP-β-CD, TMZ, their physical mixture, and inclusion complex

TMZ vesicle's existence. Moreover, the diameters of vesicles under SEM are almost the same as those in TEM images.

As shown in the inserted image in Fig. 3, a typical Tyndall effect can be seen clearly under laser in HP-β-CD/TMZ vesicles' solution. This phenomenon illustrated that there were abundant nanoparticles in HP-β-CD/TMZ sample solution [42]. Moreover, HP-β-CD/TMZ vesicles' diameters were mainly from 200 to 240 nm in DLS result. The vesicles' diameters in DLS were a little larger than the vesicles' diameters in TEM and SEM detection. This may attribute to the reason that DLS detected vesicles' hydration radius while vesicular samples in TEM and SEM were dried. Hence, DLS detection confirmed HP-β-CD/TMZ vesicles' existence as well. Those above results all give us a strong signal that HP-β-CD/TMZ vesicles can be constructed by reasonable design and preparation.

Mechanism study

XRD characterization

As shown in Fig. 4, TMZ is a typical crystal since there are many sharp peaks at 2θ including 10.8°, 14.6°, 17.9°, 19.1°, 21.5°, 26.5°, 28.9°, and 29.7° in its XRD pattern [43]. While for HP-β-CD's XRD pattern, almost no sharp peak can be seen, there are two broad peaks in the range of 5°–25°, showing an amorphous state obviously [44]. Furthermore, there are many sharp peaks in HP-β-CD/TMZ physical mixture as well, which is similar to TMZ itself. Almost all of the sharp peaks in TMZ pattern including 10.8°, 14.6°, 17.9°, 19.1°, 26.5°, 28.9°, and 29.7° and two broad peaks in the range of 5°–25° in HP-β-CD's XRD pattern existed in HP-β-CD/TMZ physical mixture, indicating that HP-β-CD/TMZ physical mixture is just a mixture of HP-β-CD and TMZ. In other words, HP-β-CD and TMZ were all in their separate initial crystal states in the physical mixture. But, compared to HP-β-

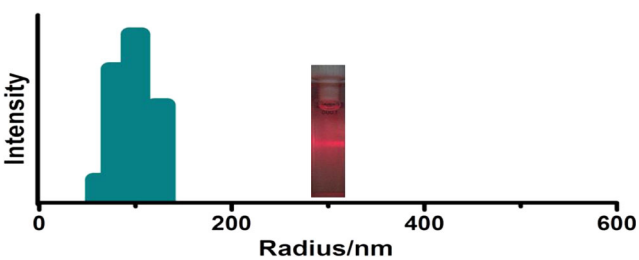

Fig. 3 HP-β-CD/TMZ vesicles' (1×10^{-4} mol/L) DLS radius distribution in water at room temperature. Inset: image of HP-β-CD/TMZ vesicles' Tyndall effect in aqueous solution

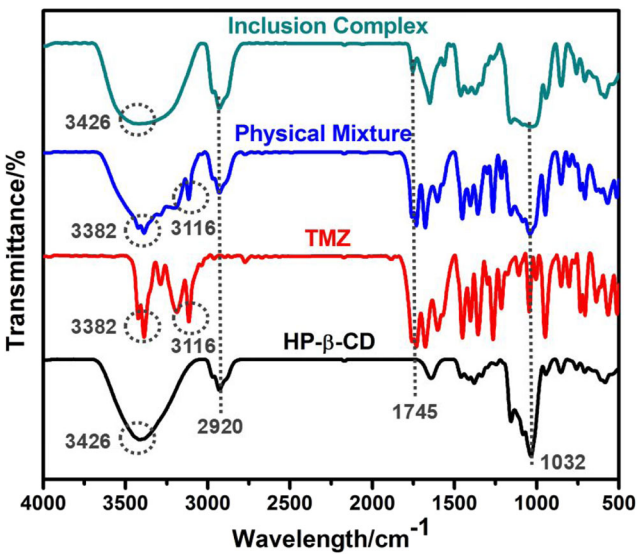

Fig. 5 FT-IR spectra comparison of HP-β-CD, TMZ, their physical mixture, and inclusion complex

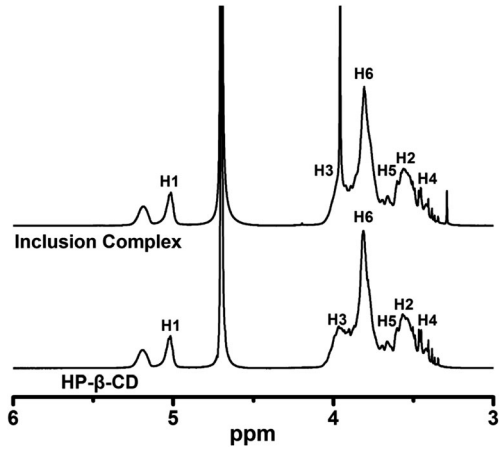

Fig. 6 ^{1}H NMR spectra comparison of HP-β-CD and HP-β-CD/TMZ sample with D_2O as the reference

CD/TMZ physical mixture, HP-β-CD/TMZ inclusion complex is very different; it shows an amorphous state since only two broad peaks in the range of 5°–25° of HP-β-CD exist while TMZ's sharp peaks almost disappear. This may be attributed to HP-β-CD/TMZ complex formation. TMZ molecule enters into the cavity of HP-β-CD molecule, leading to the disappearance of TMZ's sharp peaks.

FT-IR characterization

FT-IR, which can provide intermolecular interaction information, was used in vesicle formation mechanism exploration [45]. As shown in Fig. 5, HP-β-CD's characteristic absorption peaks ($\nu_{OH} = 3426\ cm^{-1}$, $\nu_{C\text{-}H} = 2920\ cm^{-1}$, and $\nu_{C\text{-}O\text{-}C} = 1032\ cm^{-1}$) can be found in FT-IR curves of HP-β-CD/TMZ physical mixture and HP-β-CD/TMZ inclusion complex. This illustrated that HP-β-CD existed in HP-β-CD/TMZ physical mixture and their inclusion complex. Meanwhile, TMZ's characteristic absorption peaks ($\nu_{NH} = 3382\ cm^{-1}$ and $\nu_{C=O\ of\ TMZ} = 1745\ cm^{-1}$) can be found in FT-IR curves of HP-β-CD/TMZ physical mixture and HP-β-CD/TMZ inclusion complex as well. This indicated that TMZ existed in HP-β-CD/TMZ physical mixture and their inclusion complex. However, HP-β-CD/TMZ inclusion complex pattern was different from HP-β-CD/TMZ physical mixture pattern clearly. As for HP-β-CD/TMZ physical mixture pattern, it was just like a simple overlap between HP-β-CD curve and TMZ curve. This demonstrated that HP-β-CD and TMZ molecules are relatively independent in HP-β-CD/TMZ physical mixture. However, $\nu_{NH\ of\ amido} = 3116\ cm^{-1}$ and $\nu_{C=O\ of\ TMZ} = 1745\ cm^{-1}$ of TMZ existed in HP-β-CD/TMZ physical mixture curve but almost disappeared in HP-β-CD/TMZ inclusion complex curve. This implied that HP-β-CD/TMZ inclusion complex may be in a new form by entrance of TMZ into HP-β-CD's cavity.

NMR characterizations

1H NMR characterization ^{1}H NMR is a significant tool to study interaction between different molecules [46]. The interaction of HP-β-CD and CPT was performed through 300 M ^{1}H NMR. As shown in Fig. 6 and Table 1, compared to H_2 and H_4, H_3 and H_5 protons of HP-β-CD all shifted to a higher field. Meanwhile, H_5 proton shift is highest than the other HP-β-CD protons. This suggested that TMZ molecules entered the cavities of HP-β-CD molecules under shielding effect. Meanwhile, TMZ molecule should enter the cavity of HP-β-CD molecule from the primary side rather than the second side because H_5 proton's shift is higher than H_3 proton's shift.

2D NMR characterization 2D NMR ROSEY detection was used in our study since it can give accurate evidence for

Table 1 HP-β-CD protons' shifts (Δδ) induced by the inclusion between HP-β-CD and TMZ in ^{1}H NMR

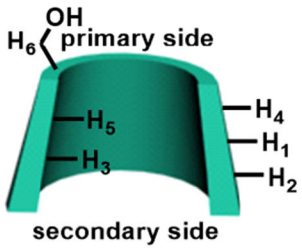

$\Delta\delta = \delta_{HP\text{-}\beta\text{-}CD} - \delta_{Complex}$

Proton	H_1	H_2	H_3	H_4	H_5	H_6
δHP-β-CD	5.0212	3.5743	3.9787	3.4719	3.6795	3.8153
δComplex	5.0199	3.5716	3.9503	3.4707	3.6504	3.8012
Δδ	0.0013	0.0027	0.0284	0.0012	0.0291	0.0141

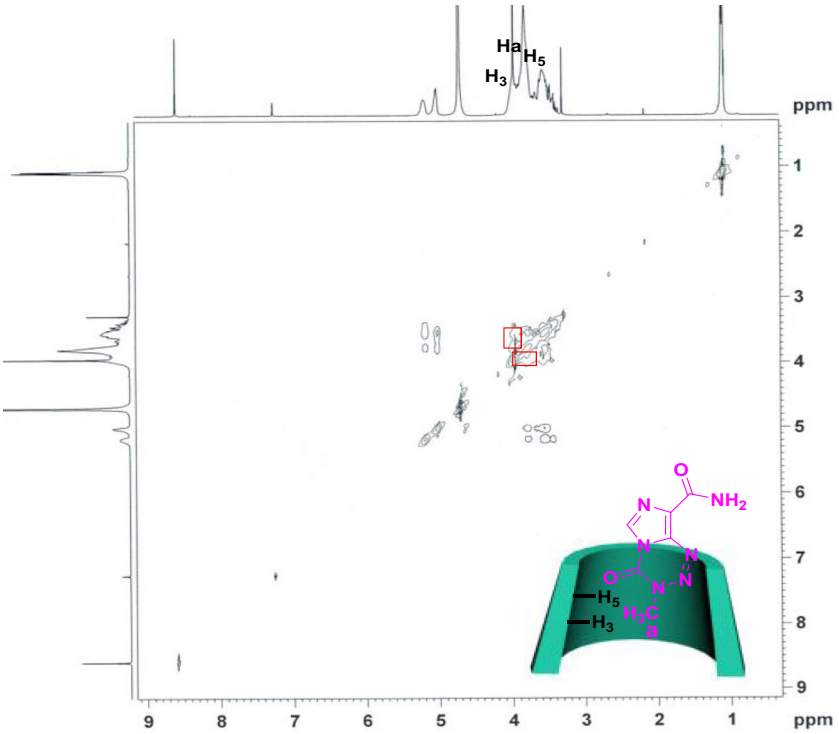

Fig. 7 2D NMR ROSEY (400 MHz) spectrum of HP-β-CD/TMZ sample with D_2O as the reference at room temperature

inclusion complex formation between host and guest molecules [47]. This detection was performed by 400 M ^{1}H NMR. As shown in Fig. 7, clear correlations between H_a of TMZ and H_3 and H_5 of HP-β-CD's inner cavity can be observed from 2D NMR ROSEY spectrum. This indicated that HP-β-CD and TMZ can form supramolecular complex through host–guest recognition. Just like ^{1}H NMR analysis, this result further confirms HP-β-CD/TMZ complex formation. The simulated diagram of HP-β-CD/TMZ complex is inserted in Fig. 7.

Detection of stoichiometry between HP-β-CD and TMZ

The stoichiometry of HP-β-CD/TMZ complex in aqueous solution can be detected through Job's plot. UV-vis spectrophotometer was used to record TMZ's absorption peaks at 266 nm with different HP-β-CD/TMZ ratios. The horizontal ordinate of Job's plot max peak was 0.5 [48] (Fig. 8). This indicated that TMZ molecule can be included by HP-β-CD molecule with 1:1 stoichiometry. Meanwhile, this result also verified that HP-β-CD can form complex with TMZ. The stoichiometry of HP-β-CD/TMZ complex can be verified by NMR detection as shown in Fig. S2. A slight upfield shift can be observed clearly for TMZ's aromatic proton with the addition of one molar HP-β-CD. However, aromatic proton of TMZ has no change with more HP-β-CD addition, illustrating HP-β-CD/TMZ complex formation with 1:1 stoichiometry. Moreover, the equilibrium binding constant of HP-β-CD/TMZ complex was determined about 0.893×10^3 M^{-1} (Fig. S3) according to the reported method [49].

The possible mechanism of the vesicular formation

From the above analysis, a reasonable mechanism of HP-β-CD/TMZ vesicle formation was proposed, as shown in

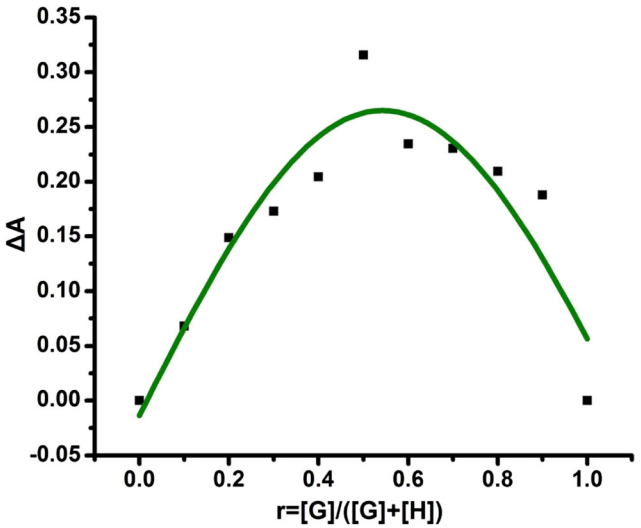

Fig. 8 Job's plot of HP-β-CD/TMZ inclusion complex in water by UV-vis detection

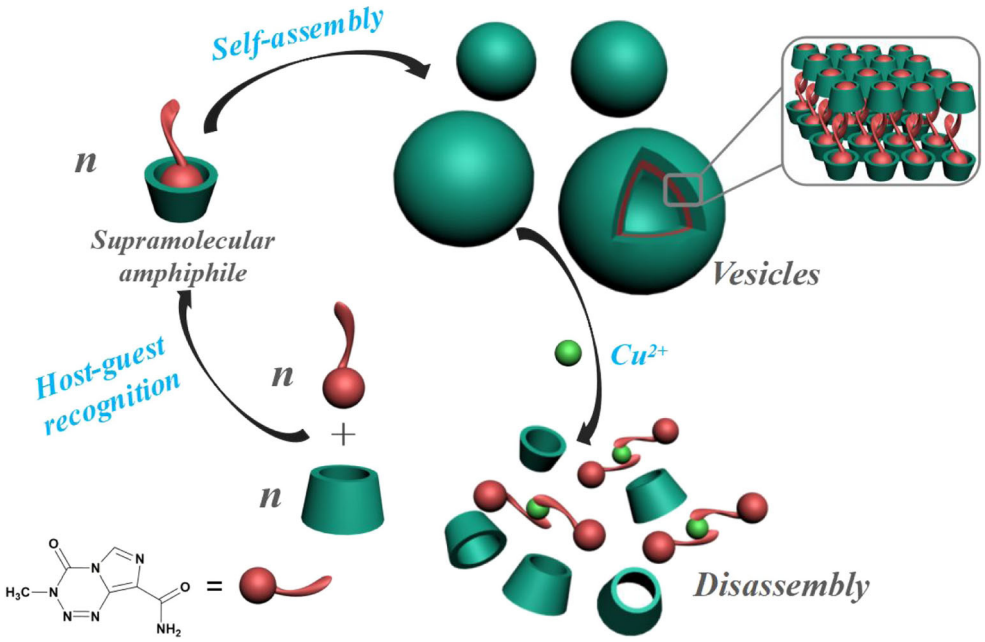

Scheme 2 The proposed mechanism of HP-β-CD/TMZ vesicle formation and its stimulus responsiveness

Scheme 2. One HP-β-CD molecule can recognize and encapsulate one TMZ molecule to form one supramolecular amphiphile through host–guest recognition. In one HP-β-CD/TMZ supramolecular amphiphile, HP-β-CD molecule is the hydrophilic, while TMZ molecule is hydrophobic. The obtained HP-β-CD/TMZ supramolecular amphiphiles can further self-assemble into vesicles by non-covalent interactions. The hydrophilic part of HP-β-CD/TMZ supramolecular amphiphile exposes to water, while the hydrophobic part of HP-β-CD/TMZ supramolecular amphiphile buries into the membrane of the vesicle to avoid water. In this way, anticancer drug TMZ can be loaded into the membranous layer of HP-β-CD/TMZ vesicles successfully.

Stimulus responsiveness of HP-β-CD/TMZ vesicles

It is reported that copper ions play an important role in cancer cell proliferation, leading to that copper ions accumulated in cancer cells are higher than those in normal cells [50]. Hence, it is necessary to study copper ions' responsiveness of HP-β-CD/TMZ vesicles. As shown in Fig. 9b, HP-β-CD/TMZ vesicle disappeared while a large number of irregular aggregates emerged when copper ions were dropped into this vesicle solution, indicating disassembly of HP-β-CD/TMZ vesicle. As shown in Scheme 2, disassembly of HP-β-CD/TMZ vesicle may be induced by coordination between copper ions and amido group of TMZ. Moreover, UV-vis detection [51] can

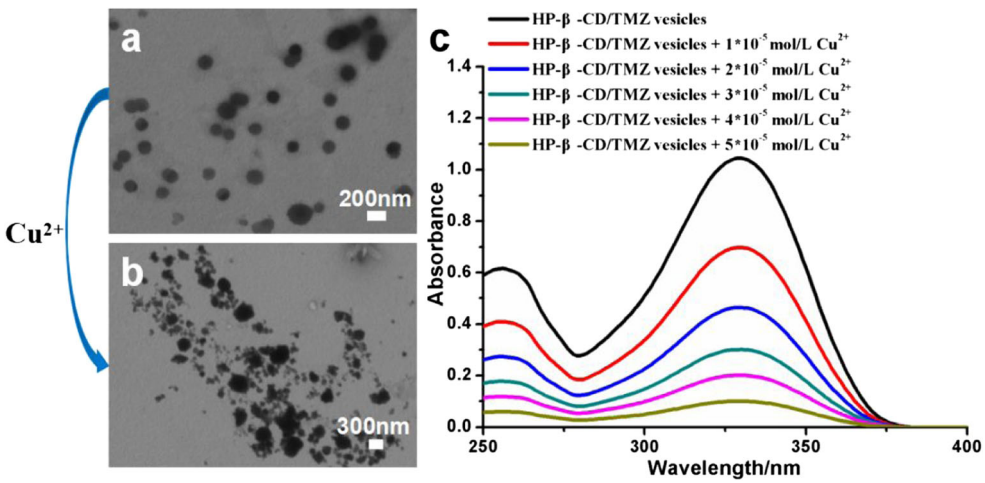

Fig. 9 (a) TEM image of the HP-β-CD/TMZ vesicle (1×10^{-4} mol/L), scale bar = 200 nm; (b) TEM image of the HP-β-CD/TMZ vesicle (1×10^{-4} mol/L) treated with copper ions (5×10^{-5} mol/L), scale bar = 300 nm; (c) UV-vis spectra comparison of HP-β-CD/TMZ vesicle and HP-β-CD/TMZ vesicle treated with different molar ratio copper ions at room temperature

further verify disassembly of HP-β-CD/TMZ vesicle since the UV-vis absorbance intensity of HP-β-CD/TMZ vesicle treated with copper ions decreased obviously than that of HP-β-CD/TMZ vesicle. So, HP-β-CD/TMZ vesicle is a smart vesicle, which can respond to copper ions sensitively, as illustrated in Scheme 2. Besides, HP-β-CD/TMZ vesicle is very sensitive to zinc ions, HP-β-CD/TMZ vesicles changed to irregular aggregates, and the UV-vis absorbance intensity of HP-β-CD/TMZ vesicles decreased clearly as well when zinc ions were added into the HP-β-CD/TMZ vesicle system (Fig. S4). But HP-β-CD/TMZ vesicle cannot respond to lithium ions since the addition of lithium ions almost did not change the morphologies and UV-vis absorbance intensity of HP-β-CD/TMZ vesicles (Fig. S5). This may be attributed to that copper ions and zinc ions have more strong complex ability with an amido group of TMZ than lithium ions. For TMZ itself, when copper ions or zinc ions were added, its UV-vis absorbance intensity reduced clearly (Fig. S6 and Fig. S7). Copper ions or zinc ions can coordinate with an amido group of TMZ, which can further decrease TMZ's UV-vis absorbance intensity.

Conclusions

In conclusion, we have successfully fabricated a supramolecular amphiphile vesicle based on HP-β-CD and TMZ. TMZ, which is the primary drug for GBM treatment, can be loaded into the membranous layer of HP-β-CD/TMZ vesicle effectively. The morphology of this vesicle was confirmed by electron microscopy. Moreover, the mechanism of vesicle formation was studied by XRD, FT-IR, UV-vis spectrum, ^{1}H NMR, and 2D NMR ROSEY. Finally, we find that HP-β-CD/TMZ vesicle can respond to copper ions sensitively. Hence, our HP-β-CD/TMZ vesicle as a smart drug delivery material may have great application potential in GBM treatment since copper ions in cancer cells are higher than those in normal cells.

Funding information This study received financial support by the Support Funds for Teachers' Scientific Research of Jining Medical University (NO. JYFC2018KJ045), PhD Start-up Scientific Research Foundation of Jining Medical University (NO. 2017JYQD03), National Natural Science Foundation of China (NO. 21872087), Shandong Science and Technology Development Plan (NO. 2016GGX107004), and Projects of Medical and Health Technology Development Program in Shandong Province (NO. 2017WS653).

Compliance with ethical standards

Conflict of interest The authors declare that they have no conflict of interest.

References

1. Patil R, Portilla-Arias J, Ding H, Inoue S, Konda B, Hu JW, Wawrowsky K, Shin P, Black K, Holler E, Ljubimova J (2010) Temozolomide delivery to tumor cells by a multifunctional nano vehicle based on poly(β-L-malic acid). Pharm Res 27:2317–2329
2. Suppasansatorna P, Wang GC, Conwaya BR, Wang WD, Wang YF (2006) Skin delivery potency and antitumor activities of temozolomide ester prodrugs. Cancer Lett 244:42–52
3. Zhang H, Gao S (2007) Temozolomide/PLGA microparticles and antitumor activity against glioma C6 cancer cells in vitro. Int J Pharm 329:122–128
4. Rosière R, Gelbcke M, Mathieu V, Antwerpen PV, Amighi K, Wauthoz N (2015) New dry powders for inhalation containing temozolomide-based nanomicelles for improved lung cancer therapy. Int J Oncol 47:1131–1142
5. Jain A, Chasoo G, Singh SK, Saxena AK, Jain SK (2011) Transferrin-appended PEGylated nanoparticles for temozolomide delivery to brain: in vitro characterisation. J Microencapsul 28: 21–28
6. Huang GH, Zhang N, Bi XL, Dou MJ (2008) Solid lipid nanoparticles of temozolomide: potential reduction of cardial and nephric toxicity. Int J Pharm 355:314–320
7. Suppasansatorn P, Nimmannit U, Conway BR, Du LR, Wang YF (2007) Microemulsions as topical delivery vehicles for the antimelanoma prodrug, temozolomide hexyl ester (TMZA-HE). J Pharm Pharmacol 59:787–794
8. Swaminathan S, Cavalli R, Trotta F (2016) Cyclodextrin-based nanosponges: a versatile platform for cancer nanotherapeutics development. WIREs Nanomed Nanobiotechnol 8:579–601
9. Appel E, Rowland MJ, Loh XJ, Heywood RM, Wattsbc C, Scherman OA (2012) Enhanced stability and activity of temozolomide in primary glioblastoma multiforme cells with cucurbit [n] uril. Chem Commun 48:9843–9845
10. Nordling-David MM, Yaffe R, Guez D, Meirow H, Last D, Grad E, Salomon S, Sharabi S, Levi-Kalisman Y, Golomb G, Mardor Y (2017) Liposomal temozolomide drug delivery using convection enhanced delivery. J Control Release 261:138–146
11. Cao Y, Hu XY, Li Y, Zou XC, Xiong SH, Lin C, Shen YZ, Wang LY (2014) Multistimuli-responsive supramolecular vesicles based on watersoluble pillar[6] arene and SAINT complexation for controllable drug release. J Am Chem Soc 136:10762–10769
12. Wang YP, Ma N, Wang ZQ, Zhang X (2007) Photocontrolled reversible supramolecular assemblies of an azobenzene-containing surfactant with a-Cyclodextrin. Angew Chem Int Ed 46:2823–2826
13. Sun T, Wang QB, Bi YK, Chen XL, Liu LS, Ruan CH, Zhao ZF, Jiang C (2017) Supramolecular amphiphiles based on cyclodextrin and hydrophobic drugs. J Mater Chem B 5:2644–2654
14. Xing PY, Sun T, Hao AY (2013) Vesicles from supramolecular amphiphiles. RSC Adv 3:24776–24793
15. Spulber M, Najer A, Winkelbach K, Glaied O, Waser M, Pieles U, Meier W, Bruns N (2013) Photoreaction of a hydroxyalkyphenone with the membrane of Polymersomes: a versatile method to generate semipermeable nanoreactors. J Am Chem Soc 135:9204–9212
16. Gao XP, Lu F, Dong B, Zhou T, Tian WF, Zheng LQ (2014) Zwitterionic vesicles with AuCl4 counterions as soft templates for the synthesis of gold nanoplates and nanospheres. Chem Commun 50:8783–8786
17. Stano P, Aguanno E, Bolz J, Fahr A, Luisi P (2013) A remarkable self-organization process as the origin of primitive functional cells. Angew Chem Int Ed 52:13397–13400
18. Zhang HC, Ma X, Nguyen KT, Zhao YL (2013) Biocompatible pillararene-as sembly-based carriers for dual bioimaging. ACS Nano 7:7853–7863

19. Wang LG, Chierico L, Little D, Patikarnmonthon N, Yang Z, Azzouz M, Madsen J, Armes S, Battaglia G (2012) Encapsulation of biomacromolecules within polymersomes by electroporation. Angew Chem Int Ed 51:11122–11125
20. Tao W, Liu Y, Jiang BB, Yu SR, Huang W, Zhou YF, Yan DY (2012) A linear-hyperbranched supramolecular amphiphile and its selfassembly into vesicles with great ductility. J Am Chem Soc 134: 762–764
21. Wang MF, Mohebbi AR, Sun YM, Wudl F (2012) Ribbons, vesicles, and baskets: supramolecular assembly of a coil-plate-coil emeraldicene derivative. Angew Chem Int Ed 51:6920–6924
22. Wang C, Guo YS, Wang YP, Xu HP, Wang RJ, Zhang X (2009) Supramolecular amphiphiles based on a water-soluble chargetransfer complex: fabrication of ultralong nanofibers with tunable straightness. Angew Chem Int Ed 48:8962–8965
23. Wang C, Yin SC, Chen SL, Xu HP, Wang ZQ, Zhang X (2008) Controlled self-assembly manipulated by charge-transfer interactions: from tubes to vesicles. Angew Chem Int Ed 47:9049–9052
24. Wang YP, Han P, Xu HP, Wang ZQ, Zhang X, Kabanov AV (2010) Photocontrolled self-assembly and disassembly of block ionomer complex vesicles: a facile approach toward supramolecular polymer nanocontainers. Langmuir 26:709–715
25. Li L, Rosenthal M, Zhang H, Hernandez JJ, Drechsler M, Phan KH, Rütten S, Zhu XM, Ivanov DA, Möller M (2012) Light-switchable vesicles from liquid-crystalline homopolymer-surfactant complexes. Angew Chem Int Ed 51:11616–11619
26. Guo DS, Wang K, Wang YX, Liu Y (2012) Cholinesterase-responsive supramolecular vesicle. J Am Chem Soc 134:10244–10250
27. Yan Q, Yuan JY, Cai ZN, Xin Y, Kang Y, Yin YW (2010) Voltage-responsive vesicles based on orthogonal assembly of two homopolymers. J Am Chem Soc 132:9268–9270
28. Duan QP, Cao Y, Li Y, Hu XY, Xiao TX, Lin C, Pan Y, Wang LY (2013) pH-responsive supramolecular vesicles based on water-soluble pillar[6] arene and ferrocene derivative for drug delivery. J Am Chem Soc 135:10542–10549
29. Ma MF, Guan Y, Zhang C, Hao JC, Xing PY, Su J, Li SY, Chu XX, Hao AY (2014) Stimulus-responsive supramolecular vesicles with effective anticancer activity prepared by cyclodextrin and ftorafur. Colloids Surf A Physicochem Eng Asp 454:38–45
30. Rui LL, Liu LC, Wang Y, Gao Y, Zhang WA (2016) Orthogonal approach to construct cell-like vesicles via pillar[5]arene-based amphiphilic supramolecular polymers. ACS Macro Lett 5:112–117
31. Wang K, Guo DS, Wang X, Liu Y (2011) Multistimuli responsive supramolecular vesicles based on the recognition of p-sulfonatocalixarene and its controllable release of doxorubicin. ACS Nano 5:2880–2894
32. Sun T, Guo Q, Zhang C, Hao JC, Xing PY, Su J, Li SY, Hao AY, Liu GC (2012) Self-assembled vesicles prepared from amphiphilic cyclodextrins as drug carriers. Langmuir 28:8625–8636
33. Sun T, Yan H, Liu GC, Hao JC, Su J, Li SY, Xing PY, Hao AY (2012) Strategy of directly employing paclitaxel to construct vesicles. J Phys Chem B 116:14628–14636
34. Xing PY, Chu XX, Li SY, Hou YH, Ma MF, Yang JS, Hao AY (2013) Self-recovering β-cyclodextrin gel controlled by good/poor solvent environments. RSC Adv 3:22087–22094
35. Liu WQ, Samanta SK, Smith BD, Isaacs L (2017) Synthetic mimics of biotin/(strept) avidin. Chem Soc Rev 46:2391–2403
36. Zhou CC, Cheng XH, Zhao Q, Yan Y, Wang JD, Huang JB (2013) Self-assembly of channel type β-CD dimers induced by dodecane. Sci Rep 4:7533–7358
37. Ma MF, Su J, Sheng X, Su F, Li SY, Xing PY, Hao AY (2014) Rapid regio- and enantioselectivities and kinetic resolution of DL-lysine by an effective supramolecular system in water. J Mol Liq 198:1–4
38. Xu L, Zhang WY, Cai HB, Liu F, Wang Y, Gao Y, Zhang WA (2015) Photocontrollable release and enhancement of photodynamic therapy based on host-guest supramolecular amphiphiles. J Mater Chem B 3:7417–7426
39. Shen QX, Liu LC, Zhang WA (2014) Fabrication of a photocontrolled surface with switchable wettability based on host-guest inclusion complexation and protein resistance. Langmuir 30:9361–9369
40. Jun SW, Kim M, Kim J, Park HJ, Lee S, Woo J, Hwang S (2007) Preparation and characterization of simvastatin/hydroxypropyl-β-cyclodextrin inclusion complex using supercritical antisolvent (SAS) process. Eur J Pharm Biopharm 66:413–421
41. Yu GC, Han CY, Zhang ZB, Chen JZ, Yan XZ, Zheng B, Liu SY, Huang FH (2012) Pillar[6]arene-based photoresponsive host-guest complexation. J Am Chem Soc 134:8711–8717
42. Yu GC, Zhou XY, Zhang ZB, Han CY, Mao ZW, Gao CY, Huang FH (2012) Pillar[6]arene/paraquat molecular recognition in water: high binding strength, pH-responsiveness, and application in controllable self-assembly, controlled release, and treatment of paraquat poisoning. J Am Chem Soc 134:19489–19497
43. Ma MF, Shang WQ, Xing PY, Li SY, Chu XX, Hao AY, Liu GC, Zhang YM (2015) A supramolecular vesicle of camptothecin for its water dispersion and controllable release. Carbohydr Res 402:208–214
44. Yang B, Lin J, Chen Y, Liu Y (2009) Artemether/hydroxypropyl-β-cyclodextrin host-guest system: characterization, phase-solubility and inclusion mode. Bioorg Med Chem 17:6311–6317
45. Li G, McGown L (1994) Molecular nanotube aggregates of β-and γ-cyclodextrins linked by diphenylhexatrienes. Science 264:249–251
46. Hou XS, Ke CF, Cheng CY, Song N, Blackburn A, Sarjeant A, Botros Y, Yang YW, Stoddart JF (2014) Efficient syntheses of pillar[6]arene-based hetero[4] rotaxanes using a cooperative capture strategy. Chem Commun 50:6196–6199
47. Sun T, Ma MF, Yan H, Shen J, Su J, Hao AY (2013) Vesicular particles directly assembled from the cyclodextrin/UR-144 supramolecular amphiphiles. Colloids Surf A Physicochem Eng Asp 424:105–112
48. An W, Zhang HC, Sun LZ, Hao AY, Hao JC, Xin FF (2010) Reversible vesicles based on one and two head supramolecular cyclodextrin amphiphile induced by methanol. Carbohydr Res 345:914–921
49. Sun HY, Bai Y, Zhao MG, Hao AY, Xu GY, Shen J, Li JY, Sun T, Zhang HC (2009) New cyclodextrin derivative 6-O-(2-hydroxybutyl)-β-cyclodextrin: preparation and its application in molecular binding and recognition. Carbohydr Res 344:1999–2004
50. Wang J, Luo C, Shan CL, You QC, Lu JY, Elf S, Zhou Y, Wen Y, Vinkenborg JL, Fan J, Kang H, Lin RT, Han DL, Xie YX, Karpus J, Chen SJ, Ouyang S, Luan CH, Zhang NX, Ding H, Merkx M, Liu H, Chen J, Jiang HL, He C (2015) Inhibtion of human copper trafficking by a small molecule significantly attenuates cancer cell proliferation. Nat Chem 7:968–979
51. Zhang Y, Swaminathan S, Tang SC, Garcia-Amoros J, Boulina M, Captain B, Baker J, Raymo FM (2015) Photoactivatable BODIPYs designed to monitor the dynamics of supramolecular nanocarriers. J Am Chem Soc 137:4709–4719